Engineering and Technology Journal
Journal homepage: https://etj.uotechnology.edu.iq

Non-linear finite element analysis for the verification and parametric study of reinforced concrete beams strengthened in compression zone to improve ductility by using ABAQUS

Dunyazad K. Assi*

Civil Engineering Dept., College of Engineering, University of Sulaimani, Sulaymaniyah, KRG-Iraq.
*Corresponding author Email: dunyazad.assi@univsul.edu.iq

HIGHLIGHTS

- The FE model accurately predicted the behavior of reinforced concrete beams compared to test results.
- Adding SF, SPHF, and hybrid (SF+CNTs) significantly enhanced ductile failure behavior.
- Carbon nanotubes have exceptional tensile strength, ranging from 50–500 GPa for SWCNTs and 10–60 GPa for MWCNTs.

Keywords:

FE-modelling

RC-beams

Ductility

Carbon nanotubes CNTs

SPFC

GFRP

ABSTRACT

Ductility is an important mechanical property of concrete structures, in tensile members, as it is the property that allows the structural member to deform plastically long before the failure point. To increase the deformation period of the beams, i.e., the ductility of failure. In the current paper, four reinforced concrete beams were modeled and compared using nonlinear finite element analysis. Reinforced concrete beams are developed and analyzed by using ABAQUS commercial software. Nonlinear material behavior, as it relates to steel reinforcing bars and plain concrete, is simulated. The effect of the change of the concrete compressive strength in the upper one-third of the beams on the ductility, the ultimate strengths, and the mode of failure of beams are investigated. One of the beam specimens was used as a reference. The change in the compressive strengths in the compressive zone was in the range of 27, 31, 37, and 42 MPa. The results of the analysis of the modeled beams were validated and compared with beams tested experimentally by previous researchers. It was found that load-deflection curves of the FE modeling of the beams match the same findings in the experiments. Furthermore, to investigate different techniques in strengthening the upper third of the beams for enhancing ultimate strength and ductility behavior, a parametric study was performed by modeling beam specimens consisting of two groups, among them using a hybrid of Carbon nanotubes (CNTs) & steel fiber, which was added to the concrete mixture of the upper third of a beam specimen and was used as strengthening layer stuck to the top layer of the compression zone of another beam. It was found that the beam that was strengthened in the compression zone by the layer of the concrete containing the mixture of the CNTs & steel fibers increased the beams' strength and ductility; hence, the ultimate load and deflection were increased by 63%, and 40%, respectively.

1. Introduction

Measures used to enhance the ductility performance of reinforced concrete elements were discussed earlier by codes and researchers. Because of increasing service loads and more stringent code stipulations, many structures are becoming functionally obsolete because the original designs no longer meet current standards; consequently, a significant number of our elements need strengthening. Among the researchers who worked on strengthening RC beams, AL-Musallam et al. [1], in addition to flexural steel reinforcement, they studied experimentally and numerically by using nonlinear finite element analysis (NFEA), the effectiveness of near-surface mounting (NSM) reinforcement bars for improving the flexural capacity of RC beams. The studied parameters included the type of NSM bars: steel versus GFR and NSM reinforcement ratio. They concluded from this investigation that the beam's flexural capacity and stiffness increase as the NSM reinforcement ratio increases to a specific limit. However, higher NSM reinforcement ratios significantly reduce deflection and energy ductility

http://doi.org/10.30684/etj.2025.157317.1912
Received 12 March 2025; Received in revised form 12 April 2025; Accepted 14 April 2025; Available online 06 May 2025
2412-0758/University of Technology-Iraq, Baghdad, Iraq

ratios. In addition, good agreement was obtained from comparing the experimental results with the FE analysis. This technique of NSM strengthening systems for improving the properties of reinforced concrete beams was also used by other researchers, including Ikram et al. [2], who used carbon fiber reinforced polymer (CFRP) strips, bars, and CFRP bars for strengthening RC beams they concluded decreasing of deflection i.e. dacoity enhancement due to the increased stiffness.

Strengthening of RC beams using unreinforced strain-hardening cementitious composites (SHCCs) layer cast to their soffit may lead to a brittle failure. So, aiming at ductility enhancement, Mohamed et al. [3], performed experimental work on RC beams that were strengthened with the SHCC layer (0.3% and 0.6% steel-reinforcement ratio). Higher strain in the strengthened layer at ultimate was recorded. Also, using a 0.6% reinforcement ratio changed the failure mode from brittle to more ductile. Zena et al. [4], performed an experimental program on simply supported beams with normal strength concrete on the compression zone and a mixture of mortar reinforced with glass fiber (FRM) was used as a part of the tension zone. Three different levels of FRM replacement were studied at 1/3, 1/2, and 2/3 of the beam thickness. It has been concluded that as the thickness of the replaced FRM increased, besides reducing the weight, the beam's toughness and ductility also increased. Dunyazad [5], used FE analysis using ABAQUS software to study the effect of using a laminate of steel propylene hybrid fibers to strengthen the shear region of beam specimens. In addition, they compared different concrete compressive strengths. The results concluded that assigning a high grade of concrete compressive strength improved the ultimate load.

However, the different types of fibers, which are dimensioned between 30 to 50 mm and 0.2 mm diameters, are used for reinforcing concrete to bridge cracks, but those fibers are not able to heal microcracks and prevent the propagation of nanoscale cracks; furthermore, the large specific area of nanomaterials enables them to fully interact with the cement matrix, and their minute size allows them to fill the nanoscale pores, within the concrete, facilitating the formation of a denser microstructure and also the control of matrix cracks at the nanoscale level.

Due to the elapsed time and cost for establishing experimental programs in a trail of studying the mechanical behavior of concrete structures, nonlinear finite element simulation became important for analyzing and predicting the mechanical behavior of reinforced concrete structures; researchers around the world are trying to develop models depending the comparison with previous experimental works among them. Hsuan et al. [6], have performed the FE analysis to study the the effect of stregthening the bottom or the two sides of beam with fiber-reinforced plastics; they concluded that the ultimate strengths and the number of cracks of the beams strengthened by FRP on both sides are much less than those strengthened by FRP at the bottom of the beams. It was also concluded that using FRP can significantly increase the stiffness.

Carbon nanotubes (CNTs) are cylindrical nanostructures of carbon atoms arranged in a hexagonal lattice; they can have single-walled (SWCNTs) or multi-walled structures (MWCNTs). Carbon nanofibers (CNFs), on the other hand, are macroscopic assemblies of aligned or entangled CNTs, resulting in a fibrous structure (Vincent et al., [7]). Among the characteristics of these materials, the tensile strength ranges between 50 and 500 GPa for SWCNTs and 10–60 GPa for MWCNTs, X [8]. CNTs exhibit exceptional mechanical, electrical, and thermal properties at the nanoscale due to their unique structure Said et al., [9].

Through extensive literature investigation about CNTs, Laura [10], stated that despite some improvement in the compressive and tensile strengths due to the incorporation of CNTs, the mechanical properties cannot constantly be improved due to their complex dispersion and low interfacial interaction with the matrix. Based on an extensive experimental program, Peng et al. [11], studied the effect of CNTs and SFs on the uniaxial concrete compressive stress-strain curve. In addition, they developed models for the pick strain, modulus of elasticity, and toughness index.

In this investigation, the nonlinear finite element was adopted by using ABAQUS software to analyze the failure behavior of reinforced concrete beams of two layers by a range of increases in the upper one-third of concrete compressive strength to enhance the ductility behavior of the RC beams. The results were compared with the test results of an experimental program performed by a previous researcher, Sawsan and Awadh [12]. Furthermore, a parametric study was conducted based on two groups of beams, aiming to improve ductility by increasing the strength of the compression zone in different ways and letting the steel in the tension zone carry the load until it reaches maximum capacity. In the first group, three beams were modeled; those beams differ from the beams that were modeled previously for verification purposes by reinforcing the upper one-third of the beams with steel fiber concrete (SFC), using steel-polypropylene hybrid (SPHF) as another variable and, using SF-carbon nanotubes (CNTS) hybrid the results were compared to the reference beam C37. In the second group, the hypotheses are based on the assumption of the probability of a stop happening after casting the bottom two-thirds of the beams, and the situation might need strengthening the remaining part of the concrete beam that must be cast after a day or any other period for completion. Such strengthening includes using fibers, additional bars in the compression zone, such as GFRP or CFRP bars, warping with CFRP sheets, and a 3cm layer consisting of a hybrid of CNTs+ SF on the top of the beam.

2. Material properties and constitutive models

This investigation was performed based on simulating beams for validation with beams tested experimentally by previous researchers mentioned in the above-forementioned section, in which the upper one-third of the beams differed from each other by their compressive strengths, which were concrete C27, C31, C37, and C42. At the same time, the lower two-thirds were made of concrete C27. A parametric study also performed consisted of two groups of beams; the first group consisted of three beams in them, the upper third was concrete C37 and different techniques was used for strengthening the upper one third of each beam in this group, in one of them SF was used and SPHF and a hybrid of (SF+CNTs) used for second and third beams, the lower two third of the beams cross section was C27. In the second group, six beams were modeled; the upper third of the

beams were concrete C20. One of the six beams was used as a reference, aiming at increasing the ductility; for the other five beams different techniques were used, such as jacketing (warping) with sheets of carbon fiber reinforced concrete (CFRC).

Moreover, in one of the modeled beams, a glass fiber reinforced (GFRP) bar is added to the compression zone (upper third layer), and in another beam, a carbon fiber reinforced concrete (CFRP) bar is used; those beams were compared to another beam specimens added steel bar to the upper third of the beam. A layer of hybrid consisted of SF and CNTs, on the top layer of the fifth beam. The materials used in the analysis are steel reinforcing bars, GFRP and CFRP, as well as a hybrid of SF and CNTS, in addition to concrete material. Reliable constitutive models applicable to these materials are used from the ABAQUS [13] material library and research.

2.1 Reinforcing steel, CFRP, and GFRP bars

The mechanical properties, such as the yielding stress of the steel reinforcing bars, were taken from experimental data for beams tested by Sawsan and Awaz [12], which was 423 MPa. Bar slipping was considered and depended on the normalization adapted by Belarbi and Hsu [14]. The stress-strain curve of the steel reinforcing bars is dependent on the elastic-plastic curve, as shown in Figure 1 (a and b).

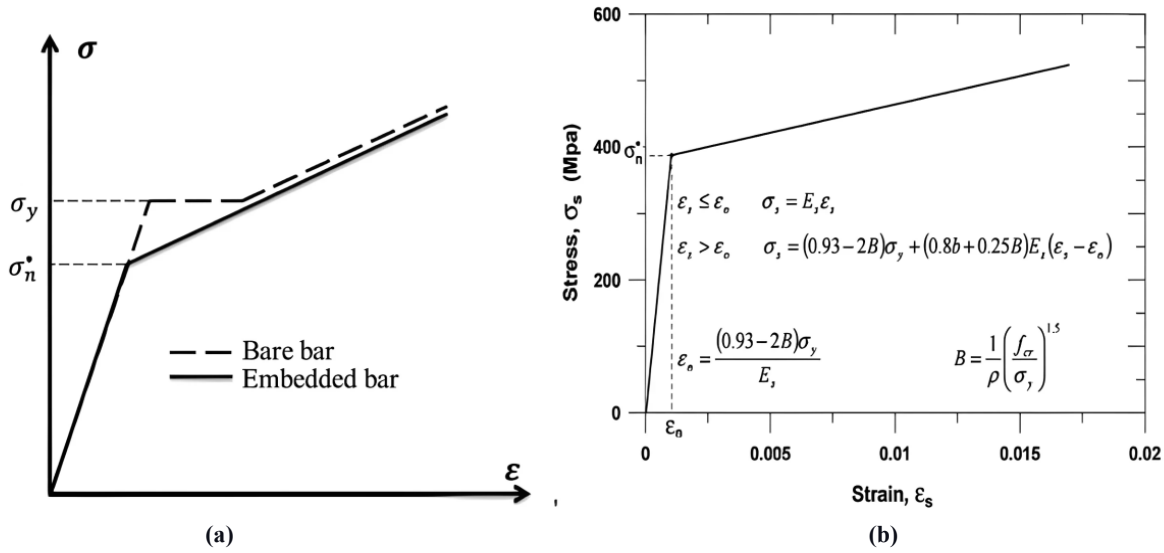

(a) **(b)**

Figure 1: Elastic perfectly plastic for steel reinforcing bar [14]

CFRP and GFRP are used as additional bars, each added to the compression zone for two different beam specimens to compare them and compare them with the beam, which used steel bars instead as an addition to the compressive zone. The properties of such kinds of bars are taken from Chellapandian [15], in which the Poisson's ratio is 0.3, and the elastic modulus is 89.4GPa and 56GPa for CFRP and GFRP bars, respectively. Figure 2a shows the simulated beam reinforced with either, CFRP or GFRP while Figure 2b shows the segmentation of the simulated beam.

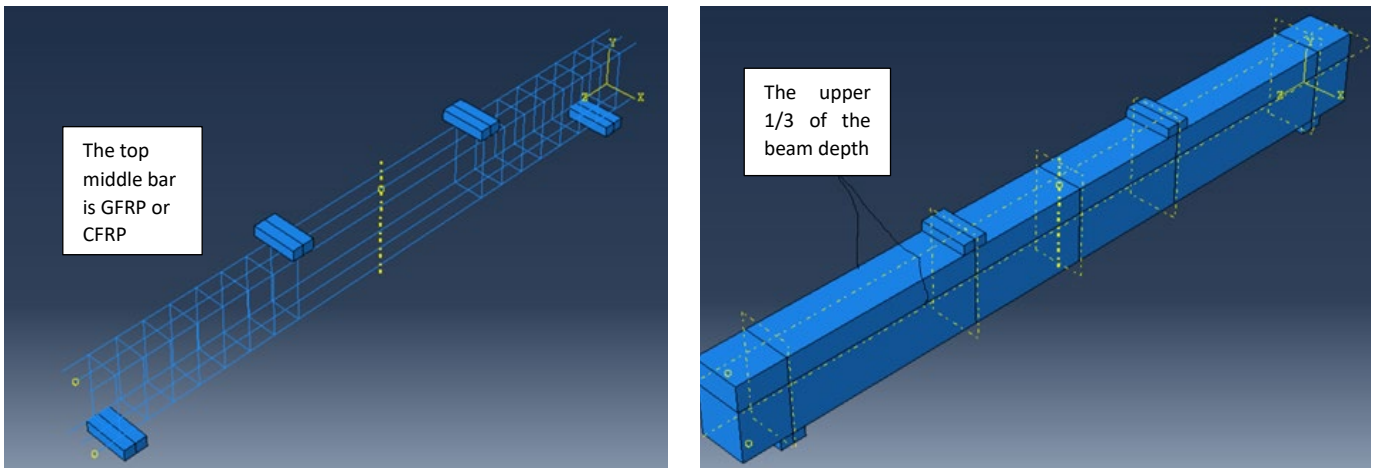

(a) **(b)**

Figure 2: The simulated beam: (a) The simulated beam reinforced with either steel, CFRP, or GFRP, (b) Segmentation of the beam in two parts, one and two-thirds of the depth

2.2 Steel-polypropylene hybrid fiber

It is well known that fibers absorb energy, increasing the toughness and ductility of failure [16-21]. This study tried to incorporate a hybrid of steel and polypropylene fiber into concrete to warp the beam, which are consisted of the concrete C20 in the upper third of the beam, as shown in Figure 3a. The properties of such fibers are taken from Yin et al. [22], in which fiber lengths was modeled as 30 mm for both of SF &PF with aspect ratio of 150 & 60 for SF&PF respectively, Ec was 25257 MPa. The reinforcing bars' stress-strain curve depends on the elastic-plastic curve adopted by the reference mentioned above, as shown below in Equations (1 and 2):

$$y = a_c x + (3 - 2a_c)x^2 + (a_c - 2)x^3 \quad 0 \le x \le 1 \tag{1}$$

$$y = \frac{x}{b_c(x-1)^2 + x} \qquad x > 1 \tag{2}$$

where y,x are the normaized stress and strain, Equation 3:

$$y = {\sigma_c^{hf}}\Big/{\sigma_{c^o}^{hf}} \ , \ x = {\varepsilon_c^{hf}}\Big/{\varepsilon_{c^o}^{hf}} \tag{3}$$

2.3 Hybrid of CNTS and steel fiber

The nanometric size of CNTs and the excellent mechanical properties of such material enhanced researchers to use it as a cement composite. Hence, in this study, A hybrid of 1.5% steel fiber and a mass fraction of 2% CNTs are mixed with the concrete C20 mixture and used as a layer of 3 cm stuck to the top fiber of the beam, as shown in Figure 3b. The mechanical properties of such hybrid were taken from Peng et al., [11]. The modulus of elasticity was dependent on the above-mentioned reference equation; E_c=2700f_c^(2⁄3) and was equal to 41380 MPa.

Based on the compressive stress-strain equations of Tomaszewicz (Equation 4) [23] and Peng et al., (Equation 5) [11], SF and CNTS were modeled in which the peak stress was 60 MPa and strain at peak stress was 0.00249.

$$\varepsilon_o = 700 \times 10^{-6} \tag{4}$$

$$y = \frac{x}{bx^3 + (1-3b)x + 2b} \tag{5}$$

where;

$$x = \frac{\varepsilon}{\varepsilon_o} \ ; \qquad y = \frac{\sigma}{f_c} \tag{6}$$

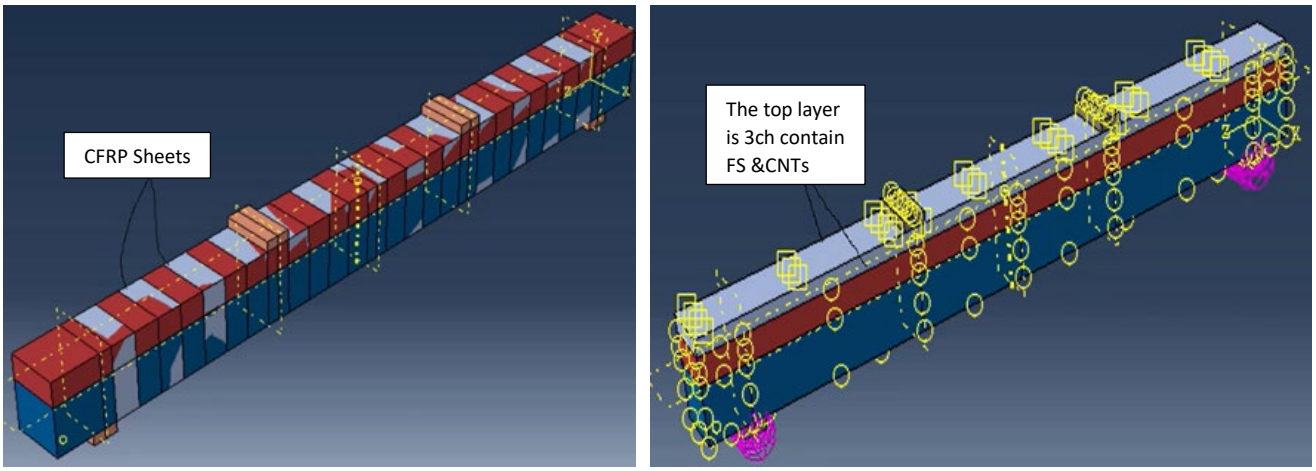

(a) **(b)**

Figure 3: Simulated beam: (a) Warped with sheets of CFRP, (b) With 3cm top layer of CNTs

2.4 Plain concrete

This study modeled four different uniaxial concrete compressive strengths, 27.6, 31.3, 37.2, and 42.4 MPa, for validation purposes. Another nine concrete beams in two groups of other variables are modeled for parametric study purposes. Concrete damage plasticity (CDP) is adapted to modeling concrete behavior; the parameters considered in the CDP are shown in Table

1. Furthermore, the concrete compressive stress strain curve for each different beam in the groups is modeled as it is mentioned in the previous Items, the tensile concrete stress-strain curve of the lower depth of the beams is dependent on the elastic-plastic curve for normal strength concrete of the Hordijk model [24].

Table 1: Concrete damage plasticity

Dilation angle	Eccentricity	Fb0/fc0	k	Viscosity
31-42	0.1	1.16	0.667	0

The uniaxial tensile strength f_t of concrete is difficult to measure, so that those values are calculated depending on the Equation 6 of ACI 318 [25].

$$f_t^{`} = 0.33\sqrt{f_c^{`}}\ MPa \tag{7}$$

The initial modulus of elasticity of concrete, *Ec,* is highly correlated to its compressive strength and can be calculated with reasonable accuracy from the empirical equation (Equation 8):

$$E_c = 4700\sqrt{f_c^{`}}\ MPa \tag{8}$$

The concrete strain (ε) corresponding to the peak stresses in compression was taken from curves adapted by Chen et al. [26], which is around 0.002. The stress-strain relationship proposed by Saenz [27], has been widely adopted as the uniaxial compressive stress-strain curve for concrete, and it has the following form.

$$\sigma_i = \frac{E_o \varepsilon_{iu}}{1+\left(R+\frac{E_o}{E_s}-2\right)\frac{\varepsilon_{iu}}{\varepsilon_{ic}}-(2R-1)\left(\frac{\varepsilon_{iu}}{\varepsilon_{ic}}\right)^2+R\left(\frac{\varepsilon_{iu}}{\varepsilon_{ic}}\right)^2} \tag{9}$$

where;

$$R = \frac{R_E\,(R_\sigma-1)}{(R_\varepsilon-1)^2}-\frac{1}{R_\varepsilon}, \qquad R_E = \frac{E_c}{E_o}\ ,\ E_o = \frac{f_c^{`}}{\varepsilon_o} \tag{10}$$

2.5 Carbon fiber reinforce dpolymer sheets (CFRP)

Sheets of CFRP with width of 100 mm was used to for warpping and the space between each was 50 mm as shown in Figure 3b. The physical and mechanical properties of the sheets used in the simulation are taken from Chellapandian [28], in which density is 1820 kg/m^3, E-value is 81.9 GPa, and tensile strength is 1188 MPa.

3. Verification of the proposed models

The validated FE models of beams are verified by previous experimental results obtained from the tests of Sawsan and Awadh [12], from which the reinforcement details and the geometric descriptions of the modeled beams are taken and provided in Tables 2 and Figure 4a. The dimensions and the reinforcement ratios were adopted as in the tested beams, the dimensions of the tested beams were 1500 mm length, 100 mm width, and 150 mm height. The longitudinal bars consisted of two and three 8-mm-diameter steel bars for compression and tension zone; consequently, the reinforcing ratio of longitudinal bars at the tension zone was 1%, and for the compression zone was 0.7%. This study considers the key variables, such as the compressive strength of the upper one-third of the beams, which was 27.6, 31.3, 37.2, and 42.4 MPa, while the lower two-thirds were 27.6 MPa for all. The two different layers of the beams that have been included in this study, which were simulated as in the experimentally tested conditions, with two different compressive strengths, are shown in Figure 4b.

Table 2: Details of the tested beams [12]

Beam Symbol	Compressive-Strength (MPa)		Flexural Reinforcement		Shear Reinforcement c/c
	Upper third	Lower two-thirds	Tension (ρ)	Compression (ρ`)	
Beam C27	27.6	27.6	3 ϕ 8	2 ϕ 8	ϕ 6 @ 60 mm
Beam C31	31.3	27.6			
Beam C37	37.2	27.6			
Beam C42	42.4	27.6			

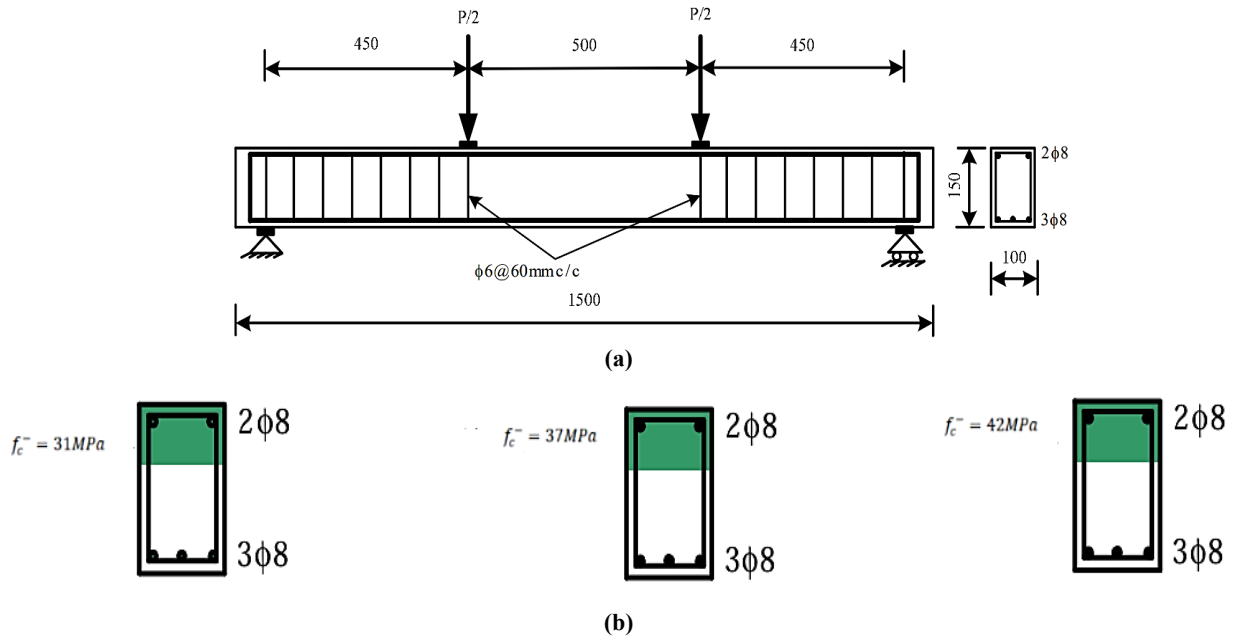

Figure 4: Details of the tested beams (all dimensions are in mm): (a) Beam profile (b) Beam sections [12]

4. Parametric study

The variables used as a parametric study in this paper consist of two groups of beams, each with the same geometry and dimension and beam layers as in the validated groups but with different variables in their upper third. In group one, three cases of concrete materials were studied; the beams were in two layers. The upper third was concrete C37; in one, SFC was used in the upper third of the beam, SPHF and CNT were used for the second and third beams, and concrete in the lower two-thirds of all of the beams was C27. The results were compared with the experimental and FE results of load defection curves of the beam C37. In group two, the idea was based on the assumption that in construction practice, in the stage of cast beams, a stope might happen in pouring concrete; after that, weaker concrete might be used for the completion casting of the beam. For that reason, and with the aim of compensating for the reduction of strength, six cases of concrete beams were proposed for investigation for strengthening. These cases are based on using the same beam condition as the beam in group one, but the upper third of the beam was simulated with a weak concrete C20, which was used as a reference beam. In another, the same beam condition but the upper third is strengthened with sheets of CFRP those sheets are warped in different places with 3mm thickness and 50 mm width, and the space of each sheet was 50 mm. The mechanical properties of the sheets are mentioned in the previous sections with steel fiber (SF). Moreover, as another variable, an extra 8mm steel bar was added to the upper third in the compressive region to increase the beam's ultimate load. The fourth and fifth beams are also simulated with an extra bar in the compressive zone, but a CFRP bar and GFRP are modeled instead of steel. As mentioned in the previous sections, despite the excellent mechanical properties of CNTs, they were not taken extensively by researchers due to the limited studies about using them in concrete due to their high cost, however, in this study they have been taken as another variable for the six beams, for strengthening the top layer of the compression zone to increase ductility of failure.

5. Results and discussion

5.1 Verification for the load-deflection relationship between the tested and simulated beams

Table 3 and Figure 5 (a-d) show the load-deflection relationships for the beams shown in which the load-deflection relationship of beam B C27 with compressive strength 27.6 MPa for both the upper and lower part of the beam geometry shown in Figure 5a demonstrates that the FE modeled curves follow the same trend as in the experimental curves; hence, the flexural strength (fr) for both of the curves nearly 24 MPa, as well as the ultimate stress (fu) for both of them are 25 MPa at a deflection of 10 mm. Therefore, it can be concluded that the FE model accurately predicts the behavior of RC beams with normal-strength concrete. Regarding the other three beams, C31, C37, and C42, there is a similarity between their fu in both test and FE results; however, there are differences in fr by increasing pertaining FE. The % increase of fr for the simulated beams C31, C37, and C42 was 20%, 13%, and 6%, respectively. That means that at the increases of compressive strengths for the upper third of the beams, the FE model matches well with the results of the tested beams. Also, there might be uncontrolled conditions about the testing conditions of the beams, such as uncontrolled deflection and slips at the beam supports, so it affects the initial loading and might lead to a small discrepancy in the results. Whereas, in the FE, those conditions are more controlled. Furthermore, the deflection for the beams for both EXP and beam C42 were increased by 80 and 140% above of the beam C27, that means increasing in ductility.

Table 3: Results of the group of the vitrificated beams

Specimen designation	f_r (MPa) for (EXP)	Deflection (mm)	f_r (MPa) for (FE)	Deflection (mm)	fu (MPa) for (Exp)	Deflection (mm)	fu (MPa) for (FE)	Deflection (mm)
B- C27	24	6	24	6	25	10	25	10
B- C31	20	5	28	5.5	28	12	27	14
B- C37	23	5.5	27	6.5	31	13.5	30	13.5
B- C42	30	7	32	7	34	18	34	24

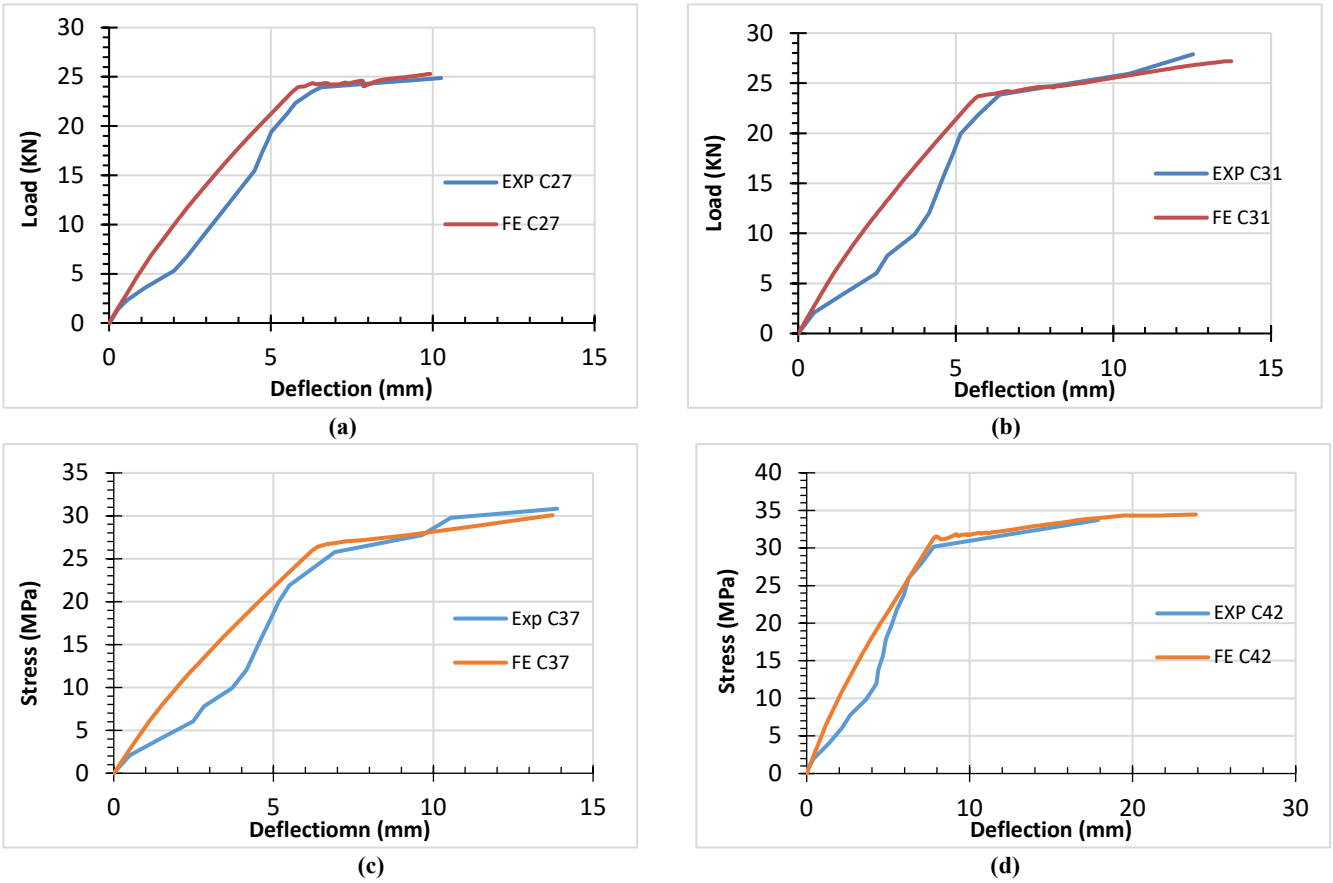

Figure 5: Load-deflection relationship for (a) beam C27, (b) beam C31 (c) beam C37, (d) beam C42

5.2 Load-deflection relationship for the two groups of beams of the parametric study

5.2.1 Load-deflection relationship for group one of the beams

Table 4 and Figure 6 show the mechanical behavior, such as fr, fu, and deflection, and load-deflection curves for four different FE-modeled beams discussed in this study. The results were compared with the load-deflection relationship of beam C37 from the experimental test. As mentioned in the previous sections, while the upper one-third of the beams has 37 MPa compressive strengths, the lower two-thirds have 27 MPa. As it is shown in the table, the result of fr for the FE modeled beam is higher than the experimentally tested beam by about 25%, and this might be due to some conditions in the experimental test was not similar to the molded one, and this is obvious because their fu result differs by 0%. So, when SF is added to the beam's top third, the fu was increased significantly by 33%, and the deflection improved by 68%, which is expected because it is well known that SF improve ductility and toughness of concrete materials.

Further increase was observed for both fr and fu in another beam when the upper one-third of the concrete beam specimen was mixed with a hybrid of 1% steel and 0.5% polypropylene fibers. Hence, in comparing with the modeled FE C37 beam, the fr was increased by 68% while the fu was increased by 50%, it has been observed that the addition of SPHF increased deflection at the fu by about 85% and this is due to the incorporation of polypropylene fiber in addition to SF. Another increase was obtained when the hybrid of 1.5% volume fraction of SF was mixed with a 2% mass fraction of CNTs and added to the concrete of the upper one-third of another beam in the group. The increase in fr and fu is 88% and 63%, respectively, and the deflection increase was 164%.

Table 4: Group one of the simulated beams

Specimen designation	EXP C37	FE C37	C37-SFC	C37-SPHF	C37-CNT
fr (MPa)	20	25	27	44	47
Deflection (mm)	5	7	9	12	13
fu (MPa)	30	30	40	45	49
Deflection (mm)	14	14	23.5	26	37

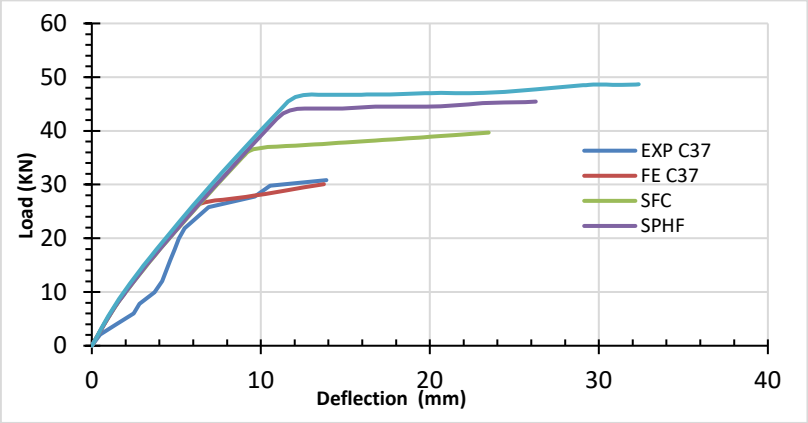

Figure 6: Load-deflection relationship for group 1 of the parametric study

5.2.2 Load-deflection relationship for group two of the beams

In a load-deflection curve for six different FE-modeled beams, as mentioned in the previous section, and shown in Figure 7, the upper one-third of the beams have 20 MPa compressive strengths, while the lower two-thirds have 27 MPa. As shown in the table of results, in this group, five different ways of strengthening, particularly in the compression zone, are investigated to compare the effect of each way on increasing the strength and flexibility of failure. Hence, different techniques were used for the upper one-third of the beams. In one of them, warping with CFRP sheets is used on another steel bar, which is added to the compression zone, and in another two FE-modeled beams, instead of using a steel bar, the CFRP bar and GFRP are added to the compression zone. Furthermore, a layer 3 cm thick hybrid consisting of CNTs and SF was cast on the top of the fifth beam. Table 5 shows the results of the fr, fu, and deflection of each of the modeled beams in this group; it is evident from the results that each technique of strengthening the top upper third of the beams is significant in increasing both fr and fu. However, strengthening with CNTs was the most valuable one. Hence, the fr, and fu increased by 40% and 63%, respectively. Moreover, the deflection was increased by 40%, and the deflection was increased by about 35%.

Table 5: Group two of the simulated beams

Specimen designation	C20	C20-CFRP Warp	C20 Steel Bar	C20-CFRP Bar	C20-GFRP Bar	CNT-SF Top layer
f_r (MPa)	22	23.5	24	24	23	31
Deflection (mm)	6	6	6	6	6	7
fu (MPa)	24	28	26	27	25	39
Deflection (mm)	13.5	17.5	15	19	15	19

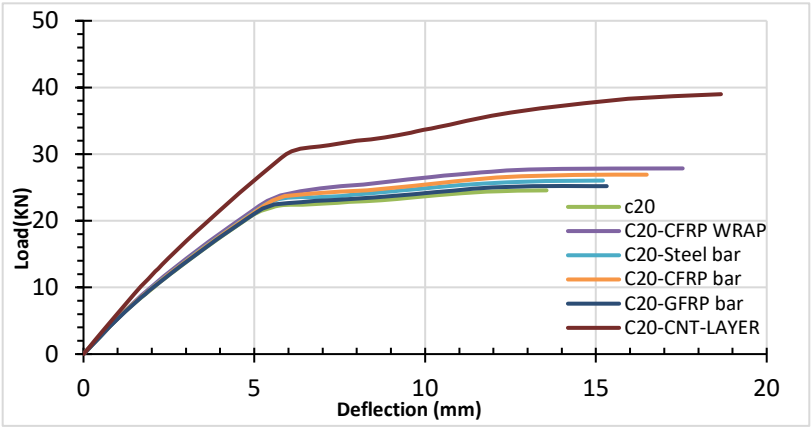

Figure 7: Load-deflection relationship for group 2 of the parametric study

6. Conclusion

In this work, nonlinear finite element analyses of RC beams depending on the group of beams were modeled and validated with the beams being tested experimentally, which was done by previous researchers, and two other groups of beams were modeled with different variables for a parametric study. Based on the numerical findings, it is concluded that:

The FE model predicts the behavior of reinforced concrete beams in close similarity with tested beams. It was observed from the results of the group validation beam increasing at increases of compressive strength at the compression zone, the ultimate load increased, and the ductility of beam C42 increased by 140% above the ductility of beam C27.

The incorporation of SF, SPHF, and a hybrid of (SF+CNTs) greatly improves the ductility of failure. However, the best of them for improving ductility was the hybrid of (SF+CNTs), in which the deflection was increased by 164%.

The group of beams consisted of two parts, the top with low-strength concrete C20 and the bottom part with concrete C27, and different techniques were used to increase the strength and ductility of failure. However, strengthening with CNTs was the most valuable one. Hence, the fr and fu increased by 41% and 63%, respectively. Moreover, the deflection was increased by 40%.

Funding

This research received no specific grant from any funding agency in the public, commercial, or not-for-profit sectors.

Data availability statement

The data that support the findings of this study are available on request from the corresponding author.

Conflicts of interest

The authors declare that there is no conflict of interest.

References

[1] A. H. Tarek, H. M. Elsanadedy, Y. A. Al-Salloum, S. H. Alsayed, Experimental and numerical investigation for the flexural strengthening of RC beams using near-surface mounted steel or GFRP bars, Constr. Build. Mater., (2013) 145-161.

[2] I. A. Saeed, S. Al-Mahaidi, T. S. Al-Attar, B. S. Al-Shathr, Flexural Behavior of RC Beams Strengthened by NSM-CFRP Laminates or Bars, Eng. Technol. J., 36 (2018) 358-367. https://doi.org/10.30684/etj.36.4A.1

[3] M. Huusain, M. Kuniedo and N. Nakamuro, Strength and ductility of RC beams strengthened with steel reinforced strain hardening cementitious composites, Cem. Concr. Compos., 34 (2012).

[4] Z. J. Yasen, A. M. Lateef and A. S. Khazaal, Structural behavior of simply supported two layers reinforced concrete (normal strength mortar and 3-dimension glass fiber), beams, Tikrit J. Eng. Sci., 28 (2021) 93- 106. https://doi.org/10.25130/tjes.28.2.08

[5] D. Assi,Verification and Parametric Analysis of Shear Behavior of Reinforced Concrete Beams using Non-linear Finite Element Analysis, J. Eng., 29 (2023) 184-202. https://doi.org/10.31026/j.eng.2023.11.11

[6] H. T. Hu, F. M. Lin, Y. Y. Jan, Non-linear finite element analysis of reinforced concrete beams strengthened by strengthened by fiber- reinforced plastics, Compos. Struct., 63 (2004) 271-281. https://doi.org/10.1016/S0263-8223(03)00174-0

[7] V. Desmaris, M. A. Saleem, S. Shafiee, Examining Carbon Nanofibers: Properties, growth, and applications, J. Mag. IEEE Nanatechnol. Mag., 9 (2015) 33-38. https://doi.org/10.1109/MNANO.2015.2409394

[8] X. L. Xie, Y. W. Mai, X. P. Zhou, Dispersion and alignment of carbon nanotubes in polymer matrix: a review, Mater. Sci. Eng. R Rep., 49 (2005) 89-112. https://doi.org/10.1016/j.mser.2005.04.002

[9] S. S. Hasan, A. Khitab, S. Ahmed, R. Arsalan, Improving mechanical performance of cement composites by addition of CNTs addition, Procedia Struct. Integrity, Elesevier Italian Group of Fracture Conference, 3 (2017) 11-17. https://doi.org/10.1016/j.prostr.2017.04.003

[10] L. Silvestro, P. J. Gleize, Effect of carbon nanotubes on compressive, flexural and tensile strengths of Portland cement-based materials: A systematic literature review, Constr. Build. Mater., 264 (2020) 120237. https://doi.org/10.1016/j.conbuildmat.2020.120237

[11] P. Zhu, Q. Jia, Z. Li, Y. Wu, Z. J. Ma, Theoretical Model for the Stress–Strain Curve of CNT-Reinforced Concrete under Uniaxial Compression, Buildings, 14 (2024) 418. https://doi.org/10.3390/buildings14020418

[12] S. A. Hassan, A. E. Ajeel, Effect of Concrete Compressive Strength and Compression Reinforcement in Compression Zone on the Ductility of Reinforced Concrete Beams, Eng. Technol. J., 32 (2016) 1106-1116. http://dx.doi.org/10.30684/etj.32.5A.2

[13] ABAQUS. Analysis of the user's manual version 2014.

[14] A. Belarbi, T. Hsu, Constitutive laws of concrete in tension and reinforcing bars stiffened by concrete, ACI Struct. J., 91 (1994) 465-474. https://doi.org/10.14359/4154

[15] C. Maheswaran, S. Prakash, A. Rajagopal, Analytical and finite element studies on hybrid FRP strengthened RC column elements under axial and eccentric compression, Comput. Struct., 184 (2017) 234-248. http://dx.doi.org/10.1016/j.compstruct.2017.09.109

[16] Y. Mohammadi, S. P. Singh, S. K. Kaushik, Properties of Steel Fibrous Concrete Containing Mixed Fibres in Fresh and Hardened State, Constr. Build. Mater., 22 (2008) 956-965. https://doi.org/10.1016/j.conbuildmat.2006.12.004

[17] Z. L. Wang, Y. S. Liu, R. F. Shen, Stress-Strain Relationship of Steel Fibre-Reinforced Concrete Under Dynamic Compression, Constr. Build. Mater., ASCE, 22 (2008) 811-819. https://doi.org/10.1016/j.conbuildmat.2007.01.005

[18] G. Giaccio, J. M. Tobes, R. Zerbino, Use of Small Beams To Obtain Design Parameters of Fibre Reinforced Concrete, Cem. Concr. Compos., 30 (2008) 297-306. https://doi.org/10.1016/j.cemconcomp.2007.10.004

[19] Z. Deng, J. Li, Mechanical Behavior of Concrete Combined with Steel and Synthetic Macro-Fibres, Int. J. Phys. Sci., 1 (2006) 57-66.

[20] D. A. Fanella, A. E. Naaman, Stress-Strain Properties of Fiber Reinforced Mortar in Compression, ACI, J., 82 (1985) 475-483. https://doi.org/10.14359/10359

[21] R. N. Swamy, The Technology of Steel Fibre Reinforced Concrete for Practical Applications, ICE Proceedings, 56 (1974) 143-159. https://doi.org/10.1680/iicep.1974.4084

[22] Y. Chi, M. Yu, L. Huang, L. Xu, Finite element modeling of steel-polypropylene hybrid fiber reinforced concrete using modified concrete damaged plasticity, Eng. Struct., 148 (2017) 23-35. https://doi.org/10.1016/j.engstruct.2017.06.039

[23] Tomaszewicz, A. Betongens Arbeidsdiagram; SINTEF REP. NO. STF 65A84605; (1984) the foundation for industrial and technical research: Trondheim, Norway.

[24] D. A. Hordijk, Tensile and tensile fatigue behavior of concrete; experiments, modelling and analyses, Heron, 37 (1992) 3-79.

[25] ACI Committee 318, Building Code Requirements for Structural Concrete (ACI 318-19) and Commentary, American Concrete Institute, Farmington Hills, MI, 2019, pp 623.

[26] Chen, Z. Y., Zhu, J. Q. and Wu, P. G. (1992), High strength concrete and its application, Beijing: Tsinghua University Press, China.

[27] P. Desayi and S. Krishnan, Equation for the stress–strain curve of concrete, J. Proce., 61 (1964) 345-350. https://doi.org/10.14359/7785

[28] M. Chellapandian, S. S.Prakash, A.Rajagopal, Analytical and finite element studies on hybrid FRP strengthened RC column elements under axial and eccentric compression, Compos. Struct., 184 (2017) 234-248. https://doi.org/10.1016/j.compstruct.2017.09.109